Published in final edited form as:
Environ Sci Technol. 2018 March 06; 52(5): 3062–3070. doi:10.1021/acs.est.7b06534.

Effects of Simulated Smog Atmospheres in Rodent Models of Metabolic and Immunologic Dysfunction

Marie McGee Hargrove[#1], **Samantha J. Snow**[#2], **Robert W. Luebke**[2], **Charles E. Wood**[2], **Jonathan D. Krug**[2], **Q. Todd Krantz**[2], **Charly King**[2], **Carey B. Copeland**[2], **Shaun D. McCullough**[2], **Kymberly M. Gowdy**[3], **Urmila P. Kodavanti**[2], **M. Ian Gilmour**[2], and **Stephen H. Gavett**[#2]

[1]Oak Ridge Institute for Science and Education, Research Triangle Park, NC 27709, USA.

[2]Office of Research and Development, U.S. Environmental Protection Agency, Research Triangle Park, NC 27711, USA.

[3]Department of Pharmacology and Toxicology, East Carolina University, Greenville, NC 27834, USA.

[#] These authors contributed equally to this work.

Abstract

Air pollution is a diverse and dynamic mixture of gaseous and particulate matter, limiting our understanding of associated adverse health outcomes. The biological effects of two simulated smog atmospheres (SA) with different compositions but similar air quality health indexes were compared in a non-obese diabetic rat model (Goto-Kakizaki, GK) and three mouse immune models (house dust mite (HDM) allergy, antibody response to heat-killed pneumococcus, and resistance to influenza A infection). In GK rats, both SA-PM (high particulate matter) and SA-O_3 (high ozone) decreased cholesterol levels immediately after a 4-hour exposure, whereas only SA-O_3 increased airflow limitation. Airway responsiveness to methacholine was increased in HDM-allergic mice compared with non-allergic mice, but exposure to SA-PM or SA-O_3 did not significantly alter responsiveness. Exposure to SA-PM did not affect the IgM response to pneumococcus, and SA-O_3 did not affect virus titers, although inflammatory cytokine levels were decreased in mice infected at the end of a 7-day exposure. Collectively, acute SA exposures produced limited health effects in animal models of metabolic and immune diseases. Effects of SA-O_3 tended to be greater than those of SA-PM, suggesting that gas-phase components in

[**]Corresponding Author: Stephen H. Gavett, Ph.D., D.A.B.T., U.S. Environmental Protection Agency, Mail Code: B105-02, Research Triangle Park, NC 27711. Telephone: (919)-541-2555; Fax: (919)-541-4715. gavett.stephen@epa.gov.

Supporting information

AQHI calculation, glucose and insulin tolerance testing, T-independent antibody titers to HKSP, and influenza A virus burden and mRNA cytokine response methods; GK rat diabetic model CBC (Table S1); mouse HDM allergy model histopathology (Table S2); indices of immunization, infection, body weights, and parameters of lung injury in mouse HKSP and influenza A models (Table S3); GK rat BALF cell numbers (Figure S1); rat BALF biochemistry (Figure S2); rat GTT, ITT results (Figure S3); mouse HDM allergy model BALF protein (Figure S4) and other biochemistry (Figure S5); mouse HDM allergy model BALF cell numbers (Figure S6); mouse HDM allergy model representative histopathology images (Figures S7, S8).

photochemically-derived multipollutant mixtures may be of greater concern than secondary organic aerosol PM.

Graphical Abstract

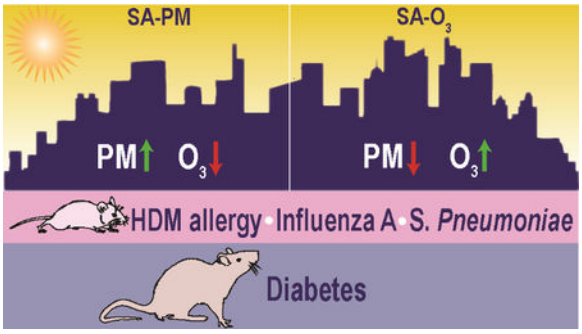

Introduction

Although air pollution toxicology has largely focused on assessments of individual air contaminants, the public is exposed to complex mixtures of pollutants with poorly-defined contributions to human health effects[1]. In 2004, the National Research Council (NRC) recommended the modification of air quality management practices to evaluate multipollutant mixtures including photochemical atmospheres[2–5]. Assessment of complex multipollutant mixtures is needed to better characterize health impacts of real-world exposures, identify sources for the most harmful pollution emissions, and enable more effective management of air quality[6]. Photochemical smog generation occurs when nitrogen oxides and volatile organic compounds (VOCs) combine in the presence of ultraviolet radiation, forming ozone (O_3), nitrogen dioxide (NO_2), secondary organic aerosols (SOAs), peroxyacetylnitrate and thousands of other compounds[7]. The health effects of photochemical smog include eye irritation, respiratory irritation, airway inflammation, and increased incidence of asthma attacks[8, 9]. These symptoms are more severe in children, the elderly and those individuals with pre-existing cardiovascular and respiratory complications. Exposure to oxidant air pollutants may alter immune responses and increase severity of respiratory viral infections[10, 11]. Recent studies have also reported that acute exposure to high O_3, a key component of photochemical smog, can lead to metabolic impairment in animal models and humans[12–14].

The principal constituents of smog such as O_3, NO_2, and SOA particulate matter (PM) may exist in differing relative concentrations as a result of regional-specific geographic and urban environment characteristics. Previous studies have modeled photochemical reactions using irradiated mixtures of hydrocarbons such as α-pinene or toluene, nitrogen oxides, and sulfur dioxide (SO_2) in rats and mice, and generally found limited effects on cardiopulmonary and vascular markers[15, 16]. Here, we generated simulated smog atmospheres (SAs) in a photochemical reaction chamber, which allows precise control of atmospheric conditions. Our objective was to study the health effects of SA mixtures with different ratios of criteria pollutants generated from ultraviolet (UV) irradiation of hydrocarbon mixtures combined

with nitric oxide (NO). Toxicological effects were evaluated in animal models of metabolic and immune disease representative of susceptible populations.

To objectively compare health effects of disparate SAs, two air quality indices were considered. The U.S. EPA Air Quality Index (AQI) is scaled from 0 to 500, where 100 typically corresponds to the national air quality standard for each pollutant[17]. AQI values >500 cannot be determined when pollutant concentrations exceed certain limits. Differing air quality standard averaging times determine pollutant concentrations used in the AQI, which is nonlinear with respect to pollution levels. Community AQI is determined by the highest individual air quality standard, and does not consider the possibility of health risks driven by multipollutant mixtures. In contrast, Health Canada's Air Quality Health Index (AQHI) quantifies health risk based on combined 3-hour average concentrations of O_3, NO_2, and $PM_{2.5}$[18]. AQHI values range from 1 (low risk) to 10 or higher (very high human health risk), and the equation for AQHI (see supporting information) allows index values >10. The ability to predict health risk at high pollutant levels using a single equation incorporating multiple criteria air pollutants led us to choose AQHI over AQI to compare health effects of complex multipollutant SAs. Our strategy was to generate SAs with very high but equivalent AQHI values driven by increased O_3 (SA-O_3) or $PM_{2.5}$ (SA-PM). These acute inhalation exposure studies were designed to investigate which dominant source profile has the greatest impact in animal models representing metabolic impairment, allergic asthma, response to immunization, or resistance to infection. Pulmonary and systemic health effects were examined in a metabolically-impaired, Type II diabetic rat model. Effects on allergic responses to house dust mite (HDM), the humoral response to immunization with heat-killed *Streptococcus pneumoniae* (HKSP), and resistance to influenza A (H1N1) infection were examined in mice. We hypothesized that exposure to simulated SAs would exacerbate health outcomes in these models of disease which would vary depending on source profile.

Materials & Methods

Generation of Simulated Smog Atmospheres

A 14.3 m^3 Teflon-coated stainless-steel mobile reaction chamber (MRC) incorporating 60 UVB and 60 sunlamps provided 300–400 nm radiation for reacting hydrocarbon mixtures. Details of chamber operation, sampling, and analysis are provided in Krug et al. in this issue[19]. Briefly, steady-state atmospheres were generated in the MRC by injecting gasoline (EPA Tier 3 standard, Southwest Research Institute, San Antonio, TX), NO, ammonium sulfate (acting as a seed aerosol for particle growth) and a supplementary biogenic component (α-pinene to promote enhanced SOA generation in SA-PM or isoprene to promote enhanced O_3 formation in SA-O_3). Atmospheres were delivered to 180 L Hinners-type chambers for whole-body rat and mouse exposures, in which animals were housed in stainless-steel individual compartments.

Rat Diabetic Model

All experimental protocols involving laboratory animals were approved by the U.S. EPA Institutional Animal Care and Use Committee. Animals were maintained in AAALAC-accredited animal facilities. Adult (15–16 weeks old, 320 ± 17 g) male Goto-Kakizaki (GK)

rats, a non-obese Type II diabetic rat model (Charles River Laboratories, Inc., Raleigh, NC), were housed individually in polycarbonate cages and received food (Rodent Chow 5001: Ralston Purina Laboratories, St. Louis, MO) and water *ad libitum*. Rats (n=6/group) were exposed to filtered air, SA-PM, or SA-O_3 4 h/d for 1 or 5 consecutive days to examine pulmonary and metabolic effects (Figure 1A).

In the 5-day exposure groups, whole-body plethysmography (WBP) was conducted to measure breathing parameters in unanesthetized unrestrained rats, which were analyzed with EMKA iox2 software (SCIREQ, Montreal, Canada). Breathing frequency, tidal volume, relaxation time, and minute volume were assessed, along with enhanced pause (Penh), a dimensionless index of airflow limitation calculated from relaxation time, peak pressures during inhalation and exhalation, and expiratory time[20]. WBP measurements (5 min) were taken pre-exposure (baseline) and immediately following the 1st, 2nd, and 4th exposures. Tests indicative of metabolic dysfunction, including glucose tolerance testing (GTT) conducted immediately following WBP measurements, and insulin tolerance testing (ITT) conducted after the 3rd exposure day, were performed according to established protocols[21] with minor alterations as detailed in the supporting information.

Rats were euthanized immediately following the 1st or 5th exposures with an overdose i.p. injection of sodium pentobarbital (> 200 mg/kg). Metabolic markers (HDL, LDL, and total cholesterol, and triglycerides) were measured in serum as previously described[22]. Plasma was collected in EDTA tubes and used to determine complete blood counts (CBC) using a Beckman-Coulter AcT blood analyzer (Beckman-Coulter Inc., Miami, FL). Bronchoalveolar lavage fluid (BALF) was collected and used to determine total cell counts, cell differentials, and the following lung injury markers: lactate dehydrogenase (LDH), protein, albumin, γ-glutamyl transferase (GGT), and *N*-acetyl-β-D-glucosaminidase (NAG), as previously described[21, 23].

Mouse HDM Allergy Model

Female BALB/cJ mice (7 weeks old, 18–21 g, Jackson Laboratories, Bar Harbor, ME) were housed 4/cage and food and water were provided *ad libitum*. On days 1 and 8 of the protocol, allergic groups were sensitized with 0.7 μg HDM extract (*Dermatophagoides pteronyssinus*, Greer Laboratories, Lenoir, NC) administered intranasally in 50 μL saline, while non-allergic groups received saline vehicle only. On day 21, all mice were challenged intranasally with 0.7 μg HDM (Figure 1B). Healthy and HDM-sensitized (allergic) mice (n=8/group) were exposed 4 h/d for 1 d (day 22) or 5 d (days 18–22) to filtered air, SA-PM, or SA-O_3. Responsiveness to methacholine (MCh) aerosol and BALF parameters were measured 2 d after HDM challenge (day 23).

One day after exposure, mice were anesthetized with urethane (1 g/kg i.p.), tracheotomized and mechanically ventilated at a rate of 150 breaths/min, tidal volume of 10 ml/kg and positive end-expiratory pressure of 2.5 cm H_2O with a small animal ventilator (flexiVent; Scireq, Montreal, Canada). Ventilated mice were injected i.p. with pancuronium bromide (0.08 mg/kg) to eliminate skeletal muscle movement. Lung resistance (R) assessing total airway constriction, and elastance (E) assessing elastic rigidity of the lungs, were determined during individual breaths with a single forced oscillation over 1 s (“snapshot”

maneuver). Three separate baseline measurements were acquired, followed by aerosolization of saline, and then increasing concentrations of MCh (5, 10, 20 and 40 mg/mL) were nebulized for 10 s into the airways, and 12 snapshot maneuvers were performed over 3 min after each nebulization. Acceptable snapshot values (goodness of fit >90%) were averaged for baselines and each dose.

Fully anesthetized mice were exsanguinated via cardiac puncture, the left lung was clamped, and the right lobes were lavaged *in situ* with HBSS (3 × 0.6 mL). BALF cell numbers and differential cell types were determined as previously described[24]. BALF supernatant was assessed for lung injury markers as described for the rat diabetic model. Left lung lobes were inflated at 20 cm pressure with 10% neutral buffered formalin. Fixed tissues were paraffin-embedded, sectioned at 5 μm, and stained with hematoxylin and eosin for histopathologic evaluation. A transverse section of each left lung lobe was evaluated by light microscopy using established pathologic criteria by a board-certified pathologist.

Mouse HKSP and Influenza A Models

Female BALB/cJ mice (6–8 weeks old, 18–21 gm, Jackson Laboratories) were housed in isolator cages supplied with fresh air from a HEPA filter system. Mice (n=10/group) were immunized or infected either immediately before the first (D1) or the last (D7) of 7 daily 4 h exposures to SA-PM (HKSP model) or SA-O_3 (influenza A model). Resource and technical issues prevented us from assessing both atmospheres in each model. This design was intended to model scenarios in which antigen or virus was introduced into an immunologically intact (D1 groups) or potentially immunocompromised (D7 groups) host. Mice were euthanized seven days after immunization or infection to assess the antibody response to immunization or clearance of virus from the lungs, respectively (Figure 1C). Body and lung lobe weights were recorded at necropsy, and BALF was collected and analyzed as described for the allergic response study.

Heat-killed *S. pneumoniae* (HKSP, Invivogen, San Diego, CA) was suspended in sterile pyrogen-free USP saline at a concentration of 8×10^8/mL. Mice were injected i.p. with 2×10^8 organisms in 0.25 mL to stimulate antibody responses to the T cell-independent antigen phosphorylcholine (PC), a component of the cell wall C-polysaccharide[25]. T helper cell-independent antibody titers to HKSP, critical to early resistance to *S. pneumoniae* infection[26], were determined using an ELISA assay developed in-house, as detailed in the supporting information.

BSL2/ABSL2 procedures were followed when infecting and working with influenza-infected animals. Mice were infected as described by Foster et al.[27], with minor modifications. Animals were anesthetized using isoflurane, and a 50 μL aliquot of sterile saline containing an estimated 300 plaque-forming units of influenza A virus (A/Puerto Rico/8/1934 (H1N1), BEI Resources, NR-28652) was deposited in the oropharyngeal cavity. Body weights were recorded daily beginning the day before infection and at necropsy and used to calculate body weight gain or loss over the course of infection. Virus burdens were estimated using real time quantitative polymerase chain reaction (qPCR) to detect copies of H1N1 polymerase acidic protein based on a method described previously[28] (see supporting information). Relative expression of selected cytokine and chemokine genes were measured

in the same lobes used to estimate virus burdens. Cytokine gene expression was assessed using commercial or synthesized primers and probes and quantified as Ct values determined using ABI 7900 real-time PCR System with SDS software 1.3.1. Change in expression was calculated using the $2^{-\Delta\Delta Ct}$ method after normalization to 18S mRNA. Ct values for exposed groups were normalized to their respective (D1 or D7) air-exposed control groups.

Statistical Analysis

Prism v. 6.0 (GraphPad Software, San Diego, CA) was used for statistical analyses of mouse allergy and rat studies. Rat plethysmography data was analyzed using repeated measures two-way ANOVA and Holm-Sidak *post-hoc* test. Mouse allergy model data were analyzed by two-way ANOVA and Tukey *post-hoc* test. Other rat data were analyzed using an unpaired t-test for each time point and atmosphere. Differences in allergy model lung lesion incidence between groups were evaluated using Fisher's Exact Test. For HKSP and virus models, SigmaPlot v. 13 (Systat Software, San Jose, CA) was used to perform two-way ANOVA followed by Holm-Sidak *post-hoc* test. All results were considered significant at $P<0.05$.

Results

SA Characterization

Measured concentrations of O_3, NO_2, and $PM_{2.5}$, along with calculated AQHI values are shown for each animal model, exposure type and duration in Table 1. For all exposures, SA-PM averaged 4.2 times more $PM_{2.5}$ than SA-O_3, while SA-O_3 averaged 3.7 times more O_3 and 2.4 times more NO_2 than SA-PM. AQHI values for all exposures averaged 100, and for each animal model there were no significant differences in AQHI between SA-PM and SA-O_3. Air control chamber O_3, NO_2, and $PM_{2.5}$ concentrations averaged less than 2 ppb, 1 ppb, and 16 μg/m^3, respectively, and relative humidity (35–45%) and temperature (72–76 °C) were equivalent for all atmospheres (data not shown).

Rat Diabetic Model

Respiratory parameters were measured using a whole-body plethysmography system to determine the effect of 5 days exposure to SA-PM or SA-O_3 on pulmonary function in the GK rat model. No changes were detected in Penh (index of airflow limitation, Figure 2A), relaxation time, breathing frequency, minute volume, or tidal volume (data not shown) following exposure to SA-PM. However, SA-O_3, which had higher levels of gaseous pollutants, led to increases in Penh (Figure 2B) after days 1 and 2 of the exposure, as well as decreases in relaxation time after day 1 of exposure. All other pulmonary functions endpoints were unaffected by SA-O_3 (data not shown).

With the exception of a slight decrease in total cells and macrophages following a 5-day exposure to SA-PM, no changes were noted in the number of BALF inflammatory cells following exposure regardless of atmosphere or time point (Figure S1). Moreover, although increased BALF protein levels in GK rats approached statistical significance (p=0.0554) following a 1-day exposure to SA-O_3, neither atmosphere resulted in significant changes to

biomarkers of pulmonary injury, including LDH, GGT, and NAG activities, or albumin and protein levels at either time point (Figure S2).

We have previously demonstrated that O_3 exposure causes metabolic impairment as indicated by elevated circulating total cholesterol, hyperglycemia, and glucose intolerance in healthy rats[21]. In the present study, a single exposure of GK rats to SA-PM resulted in significant decreases in HDL, LDL, and total cholesterols as well as triglyceride levels, while exposure to SA-O_3 led to a decrease in LDL cholesterol (Figure 3). All metabolic markers returned to baseline levels following 5 days of exposure to SA, indicating an adaptive response to the SAs. No changes were observed in hyperglycemia, glucose intolerance, or insulin intolerance following 1 to 4 days exposure to either SA (Figure S3). Furthermore, measurements of hematological parameters, platelets, and white blood cell profiles showed no significant changes regardless of exposure or time point (Table S1).

Mouse HDM Allergy Model

Lung mechanics were assessed in mice 1 day after a 5-day exposure (4 h/d) to SA-PM or SA-O_3. HDM-allergic mice were hyperresponsive to inhaled MCh compared with non-allergic mice (Figure 4). In HDM-allergic mice exposed to SA-PM, total lung resistance (Figure 4A) and elastance (Figure 4B) were significantly greater than responses in non-allergic SA-PM-exposed mice at the three highest doses of MCh. Compared with SA-PM, exposure to SA-O_3 produced fewer significant increases in resistance and elastance in HDM-allergic mice compared with non-allergic mice (Figure 4C, 4D). Overall, however, there were no significant differences in resistance or elastance between air or SA exposures in either HDM-allergic or non-allergic mice. Similarly, no changes in lung mechanics were observed 1 day after a single 4 h exposure to SA-PM or SA-O_3 (data not shown).

BALF protein levels (indicative of lung injury) were significantly increased in HDM-allergic mice exposed for 5 d to SA-O_3 in comparison with non-allergic mice exposed to air or SA-O_3, and were increased 35% (P=0.10) compared with air-exposed allergic mice (Figure S4). No significant changes were observed after a single exposure to SA-O_3, or after 1 or 5 d exposure to SA-PM. Albumin, LDH, and NAG were not significantly affected by SA-PM or SA-O_3 exposure in either HDM-allergic or non-allergic groups (Figure S5). Similarly, no significant changes were observed in numbers of BALF macrophages or neutrophils within the treatment groups following exposure to either SA (Figure S6). Significant increases in BALF eosinophils were noted within HDM-allergic mice when compared to their non-allergic controls regardless of exposure.

Independent of SA treatment, allergic sensitization resulted in an increased incidence of mixed cell inflammation in perivascular, peribronchiolar, and alveolar regions. Inflammatory cells included eosinophils, neutrophils, lymphocytes, macrophages, and in some cases rare multinucleated giant cells (Table S2). Other allergic changes included increased incidence of mucus within bronchiolar airways and mucous cell metaplasia/hyperplasia of the bronchiolar epithelium. Five days of exposure to SA-PM exposure produced an increased incidence of scant intracytoplasmic brown to black particles <2 μm in diameter within alveolar macrophages (Figure S7). In comparison to SA-PM and air-exposed mice, 5 days of exposure to SA-O_3 produced a higher incidence of minimal to mild mixed cell inflammation

(mainly perivascular) in the lungs of non-allergic mice (Table S2 and Figure S8). However, there were no significant differences in inflammation, mucus production, lymphoid hyperplasia, or other histopathological changes among HDM-allergic mice exposed to either SA in comparison to air controls.

Mouse HKSP Immunization Model

Immunization with HKSP generated T-independent anti-PC IgM antibody responses which were not affected by SA-PM exposure, nor was body weight affected in mice immunized on the first or last of the 7 exposure days (Table S3). BALF markers of inflammation and lung injury in immunized mice were comparable to historical control values and unaffected by SA-PM exposure.

Mouse Influenza A Infection Model

Compared with HKSP immunization, oropharyngeal aspiration of influenza A (IA) produced large increases in BALF markers of lung injury (LDH and protein ~5× higher) and inflammation (total cells ~10× higher) in all groups of mice, but there were no significant differences among infected mice due to exposure (air or SA-O_3) or timing (D1 *vs.* D7) of infection (Table S3). Differences in body and lung lobe weights were found which were dependent on timing of infection. Copy number of H1N1 polymerase acidic protein gene/ng of total RNA were similar in mice exposed to filtered air or SA-O_3 for 7 days, regardless of whether infection occurred prior to D1 or D7 of exposure (Figure 5A). Significant interactions in the expression of cytokine and chemokine genes occurred between the timing of infection and SA-O_3 exposure (Figure 5B). An overall reduction in inflammatory cytokine gene expression was observed in mice infected on D7 of exposure to SA-O_3, suggesting that 7 days of exposure to the O_3-enriched SA inhibited the expression of genes that play a critical role in the inflammatory response to the virus. This reduction in inflammatory cytokine gene expression was statistically significant for *Cxcl2* (chemokine (C-X-C motif) ligand 2), also known as macrophage inflammatory protein 2-alpha.

Discussion

This study was conducted to investigate the effects of two SAs with different compositions but similar air quality health indices (AQHI) in rodent models of susceptible populations. Our major findings are that: (1) a single exposure to SA-O_3 led to increases in indices of airflow obstruction in the GK rat model, including Penh at 1 and 2 days post-exposure, and decreased relaxation time, and also led to decreases in LDL cholesterol, while SA-PM did not affect lung function, but did reduce HDL and LDL cholesterol and triglyceride levels; (2) airway resistance and elastance were equivalent in HDM-allergic mice exposed to SA-PM and SA-O_3, while a trend for increased BALF protein was only observed in HDM-allergic mice exposed to SA-O_3; and (3) decreases in expression of pro-inflammatory genes (significant for *Cxcl2*) were observed after a 7-day exposure to SA-O_3 in mice infected with influenza A (H1N1) on the final day of the exposure. Overall, these findings suggest that exposure to high-ozone smog may alter metabolic, pulmonary, and immune responses in susceptible populations.

In the non-obese Type II diabetic GK rat model, the index of airflow obstruction Penh was only increased following exposure to the ozone-enriched atmosphere (SA-O_3). This finding is supported by previous studies which demonstrated an elevation in Penh levels following exposure to single gaseous-pollutant atmospheres such as O_3 and acrolein[29–31]. Penh levels returned to baseline following the 4th consecutive day of exposure, indicative of an adaptation response common with repeated O_3 exposures[32–34]. The changes noted in these breathing parameters are similar to those observed following O_3 exposure, suggesting that Penh and relaxation time may be particularly sensitive indicators of adverse pulmonary responses following smog exposure.

In contrast to prior studies showing metabolic impairment after exposure to high O_3 (800–1000 ppb) levels[12, 14], neither SA-PM nor SA-O_3, each of which contained much lower concentrations of O_3, acrolein, and PM than those used in prior single-pollutant studies[12–14, 29–31], induced hyperglycemia, glucose intolerance, or insulin resistance following exposure in the diabetic GK model. Exposures to either SA for 1 day resulted in slight decreases in serum cholesterol and triglyceride levels in GK rats. These findings contrast with prior studies where cholesterol and triglyceride levels increased after exposure to O_3 or acrolein at higher concentrations than those noted in the SA in healthy and diabetic rat models[21, 31]. Exposure to single pollutants such as O_3 also has been shown to decrease circulating white blood cell and lymphocyte numbers[35], whereas no changes in these parameters were noted after exposure to SA-PM or SA-O_3 in GK rats. Collectively, these data demonstrate that systemic responses to these relatively lower level multipollutant mixtures may differ from single pollutant exposures at high concentrations, regardless of atmosphere composition.

The HDM allergic airways disease model, in which mice are exposed to a common human allergen implicated in the development of asthma, has been used in prior studies examining the interactions of air pollution and allergens[36]. This model exhibits features of human allergic asthma, including airway hyperresponsiveness and increased BALF eosinophils and allergy-related cytokines. Since HDM allergy induces airway hyperresponsiveness to MCh aerosol, we hypothesized that exposure to airway irritants in SA may further increase lung airflow resistance in this model. Overall, MCh responsiveness in HDM-allergic mice was not significantly different among groups exposed to either SA or to air alone, indicating that the particular combination and concentrations of pollutants in these atmospheres did not further enhance irritant airway responses. Ozone concentrations in SA-O_3 averaged 376 ppb for all exposures, and 1 or 5 days of exposure did not induce hyperresponsiveness in either control or HDM-allergic mice, while O_3 at 2000 ppb for 3 h induced MCh hyperresponsiveness in rats[37] and mice[38] suggesting O_3 at a lower concentration was not sufficient to induce hyperresponsiveness even in combination with the other pollutants found in the SAs. Exposure of mice to isoprene-ozone oxidation products induced airway irritation and airflow limitation in mice, although at much higher initial isoprene and ozone concentrations than used in the present study[39, 40]. Greater sensitivity of the GK rat model in detecting airway responses compared to the mouse HDM allergy model may be due to differences in methodology. Rats were tested by WBP which detects changes in respiratory pattern in the entire respiratory tract including the nose, while mice were tested under

controlled lung ventilation, which omits contributions of the nasal passages to airflow obstruction.

The increased incidence of intracytoplasmic particles within the macrophages observed following SA-PM exposure is indicative of particle phagocytosis, consistent with previous studies utilizing PM[24]. Non-allergic mice exposed to SA-O_3 for 5-days had an increased incidence of perivascular mixed cell inflammation, although this effect was masked in SA-O_3-exposed allergic mice. A trend for increased BALF protein levels in HDM-allergic mice exposed for 5 days to SA-O_3 provided evidence of epithelial or endothelial barrier dysfunction and vascular leakage. This finding is consistent with effects in rats exposed to 0.8 ppm O_3 for 4 h, which had both increased neutrophils and protein in the lung fluid[41]. Overall, these findings suggest the alterations in pulmonary mechanics or injury within the allergic asthma mouse model depend upon the atmospheric composition.

Two separate models of immune function were included in this series of studies that assessed separate, but related, homeostatic processes. The T-independent antibody response was assessed in mice exposed to SA-PM, while resistance to influenza A infection was assessed after exposure to SA-O_3. Since mice lacking T helper cells do mount a protective T-independent antibody response when infected with influenza A[42], there is a functional continuity between the assays. There was no effect of SA exposure on apical measures of host immunocompetence (IgM antibody titers to HKSP or virus burdens), although exposure to SA-O_3 (averaging 376 ppb O_3) did affect *Cxcl2* expression, and tended to inhibit the expression of other key inflammatory response genes (Figure 5). Others have reported that exposure to 500 ppb O_3 reduced the severity of influenza infection and distribution of virus in the lung without altering virus burdens[43, 44]. Suppression of the anti-viral immune response (T and B cells, specific antibody titers) was suggested as a possible factor in reducing the severity of infection[44]. Our cytokine gene expression data are consistent with a role for O_3 in reducing the response to infection.

In summary, complex multipollutant mixtures were generated by photochemical reactions of gasoline mixed with α-pinene or isoprene, NO, and ammonium sulfate to produce SA-PM dominated by secondary organic aerosol-based PM, and SA-O_3 dominated by O_3 and NO_2. These atmospheres produced few short-term health effects in animal models of metabolic and immune diseases, although greater responses were found with SA-O_3 in respiratory responses of GK rats, BALF protein in mice, and inflammatory cytokine depression in mice exposed to influenza A virus. Additional studies are needed to characterize photochemical smog exposures which result in metabolic, cardiopulmonary, and immune dysfunction.

Supplementary Material

Refer to Web version on PubMed Central for supplementary material.

Acknowledgements

MMH was supported by interagency agreement #92429801 with the Oak Ridge Institute for Science and Education. The authors thank the following U.S. EPA scientists for their excellent assistance: Lisa Copeland, Rick Jaskot, Allen Ledbetter, David Morgan, Judy Richards, Mette Schladweiler, Wanda Williams, and Carmen Wood. We also thank Drs. Jan Dye and Mike Madden for careful review of the manuscript.

References

1. Stanek LW; Brown JS; Stanek J; Gift J; Costa DL Air pollution toxicology - a brief review of the role of the science in shaping the current understanding of air pollution health risks. Toxicol. Sci 2011, 120, (suppl 1), S8–S27. [PubMed: 21147959]
2. National Research Council, Air Quality Management in the United States. The National Academies Press: Washington, DC, 2004; 426 p. https://www.nap.edu/catalog/10728/air-quality-management-in-the-united-states.
3. U.S. EPA. The Multi-Pollutant Report: Technical Concepts and Examples: Washington, DC, 2008 https://archive.epa.gov/airquality/aqmp/web/pdf/20080702_multipoll.pdf.
4. Johns DO; Stanek LW; Walker K; Benromdhane S; Hubbell B; Ross M; Devlin RB; Costa DL; Greenbaum DS Practical advancement of multipollutant scientific and risk assessment approaches for ambient air pollution. Environ. Health Perspect 2012, 120, (9), 1238–1242. [PubMed: 22645280]
5. U.S. EPA. Moving Towards Multi-Air Pollutant Reduction Strategies in Major U.S. Industry Sectors: Washington, DC, 2011 https://www.epa.gov/sites/production/files/2014-08/documents/reduction_strategies.pdf.
6. Dominici F; Peng RD; Barr CD; Bell ML Protecting human health from air pollution: shifting from a single-pollutant to a multipollutant approach. Epidemiology 2010, 21, (2), 187–194. [PubMed: 20160561]
7. Gaffney JS; Marley NA Atmospheric chemistry and air pollution. Sci. World J 2003, 3, 199–234.
8. Gilmour MI; Jaakkola MS; London SJ; Nel AE; Rogers CA How exposure to environmental tobacco smoke, outdoor air pollutants, and increased pollen burdens influences the incidence of asthma. Environ. Health Perspect 2006, 114, (4), 627–633. [PubMed: 16581557]
9. Kurt OK; Zhang J; Pinkerton KE Pulmonary health effects of air pollution. Curr. Opin. Pulm. Med 2016, 22, (2), 138–143. [PubMed: 26761628]
10. Jakab GJ; Spannhake EW; Canning BJ; Kleeberger SR; Gilmour MI The effects of ozone on immune function. Environ. Health Perspect 1995, 103 Suppl 2, 77–89.
11. Kesic MJ; Meyer M; Bauer R; Jaspers I Exposure to ozone modulates human airway protease/antiprotease balance contributing to increased influenza A infection. PloS one 2012, 7, (4), e35108. [PubMed: 22496898]
12. Bass V; Gordon CJ; Jarema KA; MacPhail RC; Cascio WE; Phillips PM; Ledbetter AD; Schladweiler MC; Andrews D; Miller D; Doerfler DL; Kodavanti UP Ozone induces glucose intolerance and systemic metabolic effects in young and aged Brown Norway rats. Toxicol. Appl. Pharmacol 2013, 273, (3), 551–560. [PubMed: 24103449]
13. Miller DB; Ghio AJ; Karoly ED; Bell LN; Snow SJ; Madden MC; Soukup J; Cascio WE; Gilmour MI; Kodavanti UP Ozone exposure increases circulating stress hormones and lipid metabolites in humans. Am. J. Respir. Crit. Care Med 2016, 193, (12), 1382–1391. [PubMed: 26745856]
14. Vella RE; Pillon NJ; Zarrouki B; Croze ML; Koppe L; Guichardant M; Pesenti S; Chauvin M-A; Rieusset J; Géloën A; Soulage CO Ozone exposure triggers insulin resistance through muscle c-Jun N-terminal kinase activation. Diabetes 2015, 64, (3), 1011–1024. [PubMed: 25277399]
15. Lund AK; Doyle-Eisele M; Lin YH; Arashiro M; Surratt JD; Holmes T; Schilling KA; Seinfeld JH; Rohr AC; Knipping EM; McDonald JD The effects of alpha-pinene versus toluene-derived secondary organic aerosol exposure on the expression of markers associated with vascular disease. Inhal. Toxicol 2013, 25, (6), 309–324. [PubMed: 23742109]
16. McDonald JD; Doyle-Eisele M; Campen MJ; Seagrave J; Holmes T; Lund A; Surratt JD; Seinfeld JH; Rohr AC; Knipping EM Cardiopulmonary response to inhalation of biogenic secondary organic aerosol. Inhal. Toxicol 2010, 22, (3), 253–265. [PubMed: 20148748]
17. U.S. EPA. Technical Assistance Document for the Reporting of Daily Air Quality – the Air Quality Index (AQI): Research Triangle Park, NC, 2016 https://www3.epa.gov/airnow/aqi-technical-assistance-document-may2016.pdf.
18. Stieb DM; Burnett RT; Smith-Doiron M; Brion O; Shin HH; Economou V A new multipollutant, no-threshold air quality health index based on short-term associations observed in daily time-series analyses. J. Air Waste Manag. Assoc 2008, 58, (3), 435–450. [PubMed: 18376646]

19. Krug JD; Lewandowski M; Offenberg JH; Turlington JM; Lonneman WA; Modak N; Krantz QT; King C; Jaoui M; Gavett SH; Gilmour MI; DeMarini D; Kleindienst TE The photochemical conversion of surrogate emissions for use in toxicological studies: role of particulate- and gas-phase products. Environ. Sci. Technol In review.

20. Hamelmann E; Schwarze J; Takeda K; Oshiba A; Larsen GL; Irvin CG; Gelfand EW Noninvasive measurement of airway responsiveness in allergic mice using barometric plethysmography. Am. J. Respir. Crit. Care Med 1997, 156, (3 Pt 1), 766–775. [PubMed: 9309991]

21. Miller DB; Karoly ED; Jones JC; Ward WO; Vallanat BD; Andrews DL; Schladweiler MC; Snow SJ; Bass VL; Richards JE; Ghio AJ; Cascio WE; Ledbetter AD; Kodavanti UP Inhaled ozone (O3)-induces changes in serum metabolomic and liver transcriptomic profiles in rats. Toxicol. Appl. Pharmacol 2015, 286, (2), 65–79. [PubMed: 25838073]

22. Miller DB; Snow SJ; Henriquez A; Schladweiler MC; Ledbetter AD; Richards JE; Andrews DL; Kodavanti UP Systemic metabolic derangement, pulmonary effects, and insulin insufficiency following subchronic ozone exposure in rats. Toxicol. Appl. Pharmacol 2016, 306, 47–57. [PubMed: 27368153]

23. Snow SJ; McGee J; Miller DB; Bass V; Schladweiler MC; Thomas RF; Krantz T; King C; Ledbetter AD; Richards J; Weinstein JP; Conner T; Willis R; Linak WP; Nash D; Wood CE; Elmore SA; Morrison JP; Johnson CL; Gilmour MI; Kodavanti UP Inhaled diesel emissions generated with cerium oxide nanoparticle fuel additive induce adverse pulmonary and systemic effects. Toxicol. Sci 2014, 142, (2), 403–417. [PubMed: 25239632]

24. McGee MA; Kamal AS; McGee JK; Wood CE; Dye JA; Krantz QT; Landis MS; Gilmour MI; Gavett SH Differential effects of particulate matter upwind and downwind of an urban freeway in an allergic mouse model. Environ. Sci. Technol 2015, 49, (6), 3930–9. [PubMed: 25710269]

25. Wu Z-Q; Khan AQ; Shen Y; Schartman J; Peach R; Lees A; Mond JJ; Gause WC; Snapper CM B7 Requirements for Primary and Secondary Protein- and Polysaccharide-Specific Ig Isotype Responses to Streptococcus pneumoniae. J. Immunol 2000, 165, (12), 6840–6848. [PubMed: 11120807]

26. Baumgarth N The double life of a B-1 cell: self-reactivity selects for protective effector functions. Nat. Rev. Immunol 2011, 11, (1), 34–46. [PubMed: 21151033]

27. Foster WM; Walters DM; Longphre M; Macri K; Miller LM Methodology for the measurement of mucociliary function in the mouse by scintigraphy. J. Appl. Physiol 2001, 90, (3), 1111–1118. [PubMed: 11181627]

28. Jelley-Gibbs DM; Dibble JP; Brown DM; Strutt TM; McKinstry KK; Swain SL Persistent depots of influenza antigen fail to induce a cytotoxic CD8 T cell response. J. Immunol 2007, 178, (12), 7563–7570. [PubMed: 17548591]

29. Kodavanti UP; Thomas R; Ledbetter AD; Schladweiler MC; Shannahan JH; Wallenborn JG; Lund AK; Campen MJ; Butler EO; Gottipolu RR; Nyska A; Richards JE; Andrews D; Jaskot RH; McKee J; Kotha SR; Patel RB; Parinandi NL Vascular and cardiac impairments in rats inhaling ozone and diesel exhaust particles. Environ. Health Perspect 2011, 119, (3), 312–318. [PubMed: 20980218]

30. Savov JD; Whitehead GS; Wang J; Liao G; Usuka J; Peltz G; Foster WM; Schwartz DA Ozone-induced acute pulmonary injury in inbred mouse strains. Am. J. Respir. Cell Mol. Biol 2004, 31, (1), 69–77. [PubMed: 14975936]

31. Snow SJ; McGee MA; Henriquez A; Richards JE; Schladweiler MC; Ledbetter AD; Kodavanti UP Respiratory effects and systemic stress response following acute acrolein inhalation in rats. Toxicol. Sci 2017, doi: 10.1093/toxsci/kfx108.

32. Folinsbee LJ; Bedi JF; Horvath SM Respiratory responses in humans repeatedly exposed to low concentrations of ozone. Am. Rev. Respir. Dis 1980, 121, (3), 431–439. [PubMed: 7416576]

33. Tepper JS; Costa DL; Lehmann JR; Weber MF; Hatch GE Unattenuated structural and biochemical alterations in the rat lung during functional adaptation to ozone. Am. Rev. Respir. Dis 1989, 140, (2), 493–501. [PubMed: 2527482]

34. Snow SJ; Gordon CJ; Bass VL; Schladweiler MC; Ledbetter AD; Jarema KA; Phillips PM; Johnstone AF; Kodavanti UP Age-related differences in pulmonary effects of acute and subchronic episodic ozone exposures in Brown Norway rats. Inhal. Toxicol 2016, 28, (7), 313–323. [PubMed: 27097751]

35. Miller DB; Snow SJ; Schladweiler MC; Richards JE; Ghio AJ; Ledbetter AD; Kodavanti UP Acute ozone-induced pulmonary and systemic metabolic effects are diminished in adrenalectomized rats. Toxicol. Sci 2016, 150, (2), 312–322. [PubMed: 26732886]
36. Gavett SH; Wood CE; Williams MA; Cyphert JM; Boykin EH; Daniels MJ; Copeland LB; King C; Krantz TQ; Richards JH; Andrews DL; Jaskot RH; Gilmour MI Soy biodiesel emissions have reduced inflammatory effects compared to diesel emissions in healthy and allergic mice. Inhal. Toxicol 2015, 27, (11), 533–544. [PubMed: 26514781]
37. Sunil VR; Vayas KN; Massa CB; Gow AJ; Laskin JD; Laskin DL Ozone-induced injury and oxidative stress in bronchiolar epithelium are associated with altered pulmonary mechanics. Toxicol. Sci 2013, 133, (2), 309–319. [PubMed: 23492811]
38. Kasahara DI; Mathews JA; Park CY; Cho Y; Hunt G; Wurmbrand AP; Liao JK; Shore SA ROCK insufficiency attenuates ozone-induced airway hyperresponsiveness in mice. Am. J. Physiol. Lung Cell. Mol. Physiol 2015, 309, (7), L736–L746. [PubMed: 26276827]
39. Rohr AC; Shore SA; Spengler JD Repeated exposure to isoprene oxidation products causes enhanced respiratory tract effects in multiple murine strains. Inhal. Toxicol 2003, 15, (12), 1191–1207. [PubMed: 14515222]
40. Rohr AC; Wilkins CK; Clausen PA; Hammer M; Nielsen GD; Wolkoff P; Spengler JD Upper airway and pulmonary effects of oxidation products of (+)-alpha-pinene, d-limonene, and isoprene in BALB/c mice. Inhal. Toxicol 2002, 14, (7), 663–684. [PubMed: 12122569]
41. Bouthillier L; Vincent R; Goegan P; Adamson IY; Bjarnason S; Stewart M; Guenette J; Potvin M; Kumarathasan P Acute effects of inhaled urban particles and ozone: lung morphology, macrophage activity, and plasma endothelin-1. Am. J. Pathol 1998, 153, (6), 1873–1884. [PubMed: 9846977]
42. Lee BO; Rangel-Moreno J; Moyron-Quiroz JE; Hartson L; Makris M; Sprague F; Lund FE; Randall TD CD4 T cell-independent antibody response promotes resolution of primary influenza infection and helps to prevent reinfection. J. Immunol 2005, 175, (9), 5827–5838. [PubMed: 16237075]
43. Wolcott JA; Zee YC; Osebold JW Exposure to ozone reduces influenza disease severity and alters distribution of influenza viral antigens in murine lungs. Appl. Environ. Microbiol 1982, 44, (3), 723–731. [PubMed: 6182839]
44. Jakab GJ; Hmieleski RR Reduction of influenza virus pathogenesis by exposure to 0.5 ppm ozone. J Toxicol. Environ. Health 1988, 23, (4), 455–472. [PubMed: 3361616]

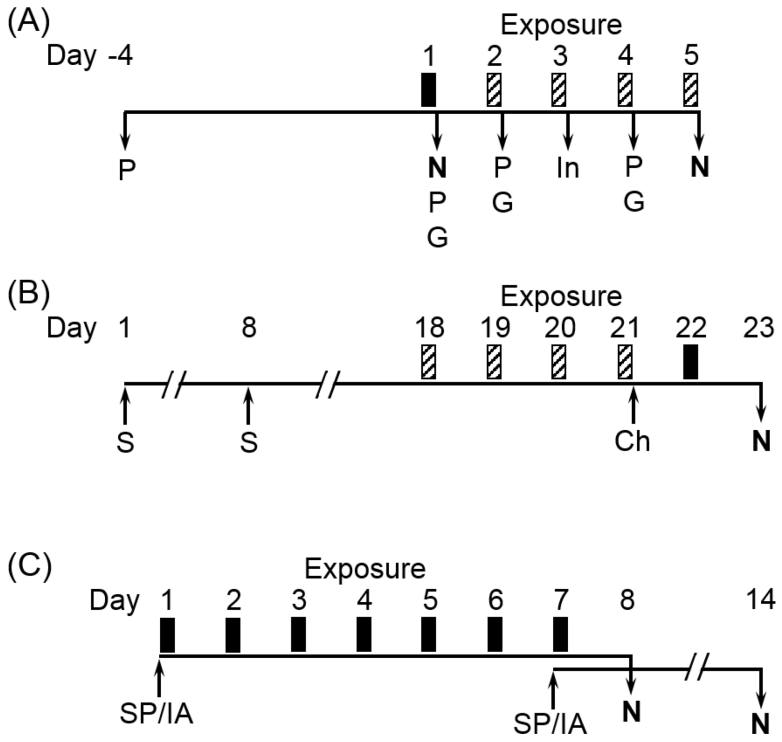

Figure 1.

Experimental designs for studies examining effects of simulated smog atmospheres (SA) on animal models of metabolic and immune disease. (A) GK rats were exposed for 4 h to either SA-PM (high PM) or SA-O_3 (high O_3) for 1 d (solid bar) or 5 d (solid and striped bars). Rats exposed for 5 d were assessed for pulmonary function (P), glucose tolerance testing (G), and insulin tolerance testing (In) immediately after exposure on indicated days. Rats were necropsied (N) immediately after 1 or 5 d of exposure. (B) Balb/cJ mice were sensitized (S) and challenged (Ch) with HDM on indicated days. Mice were exposed for 4 h to either SA-PM or SA-O_3 for 1 d (solid bar) or 5 d (solid and striped bars). One day after the final exposure, mice were assessed for airway responses to methacholine challenge and necropsied (N) to assess allergic endpoints. (C) The immune response to heat-killed *Streptococcus pneumoniae* (SP) was tested in Balb/cJ mice exposed for 7 d (4 h/d) to SA-PM, and the response to influenza A (IA) infection was tested in mice exposed for 7 d (4 h/d) to SA-O_3. Mice were immunized with SP or infected with IA immediately prior to the first or last day of SA exposure, and all mice were necropsied (N) 7 d after immunization or infection.

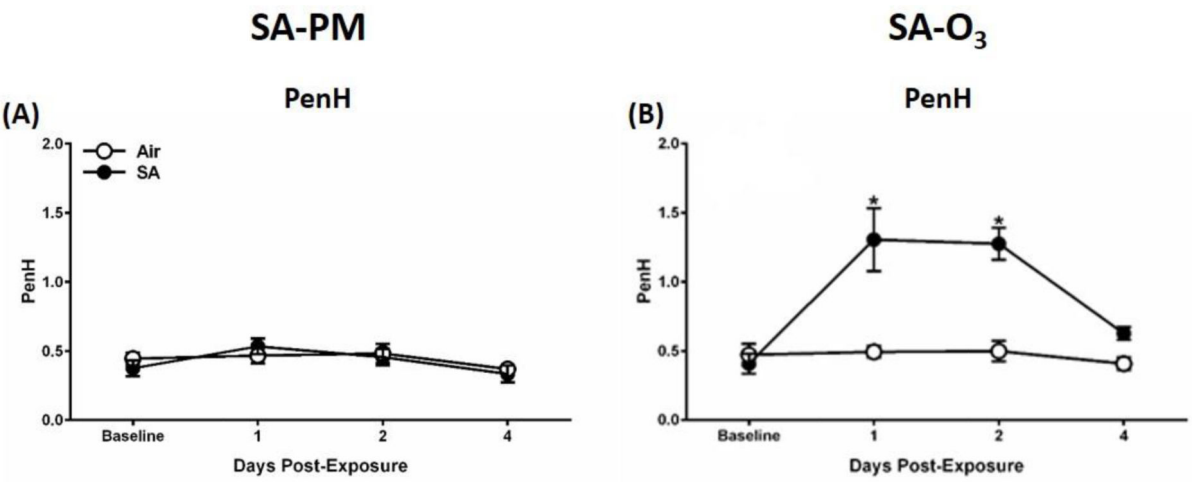

Figure 2.

$SA\text{-}O_3$ alters pulmonary function in GK diabetic rats. Whole-body plethysmography was performed on GK rats following exposure to filtered air, SA-PM (panel A), or $SA\text{-}O_3$ (panel B). Measurements for Penh were taken at baseline prior to exposure and immediately following the 1^{st}, 2^{nd}, and 4^{th} exposures in the 5-day groups. Data show mean ± SEM (n=6/group). *$P<0.05$ *vs.* filtered air exposure group at that time point.

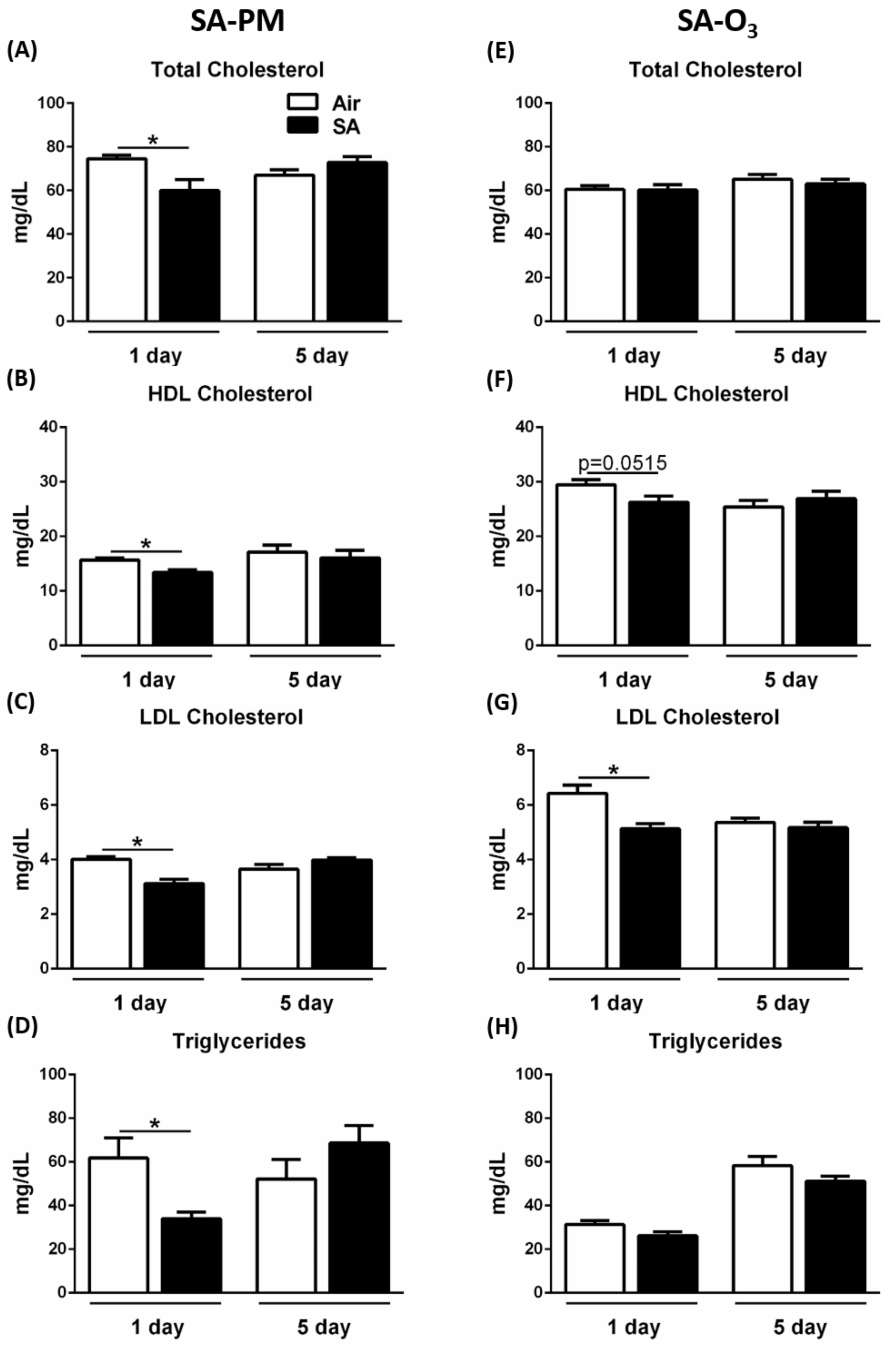

Figure 3.

SAs reduce cholesterol and triglyceride levels at 1 day post-exposure in GK rats. Metabolic markers were measured in GK rats following exposure to filtered air, SA-PM (left panels), or SA-O_3 (right panels) for 1 day or 5 consecutive days. Serum samples were analyzed for total cholesterol (A, E), HDL cholesterol (B, F), LDL cholesterol (C, G), and triglycerides (D, H). Data show mean ± SEM (n=6/group). **P*<0.05 significantly different than filtered air group at that time point.

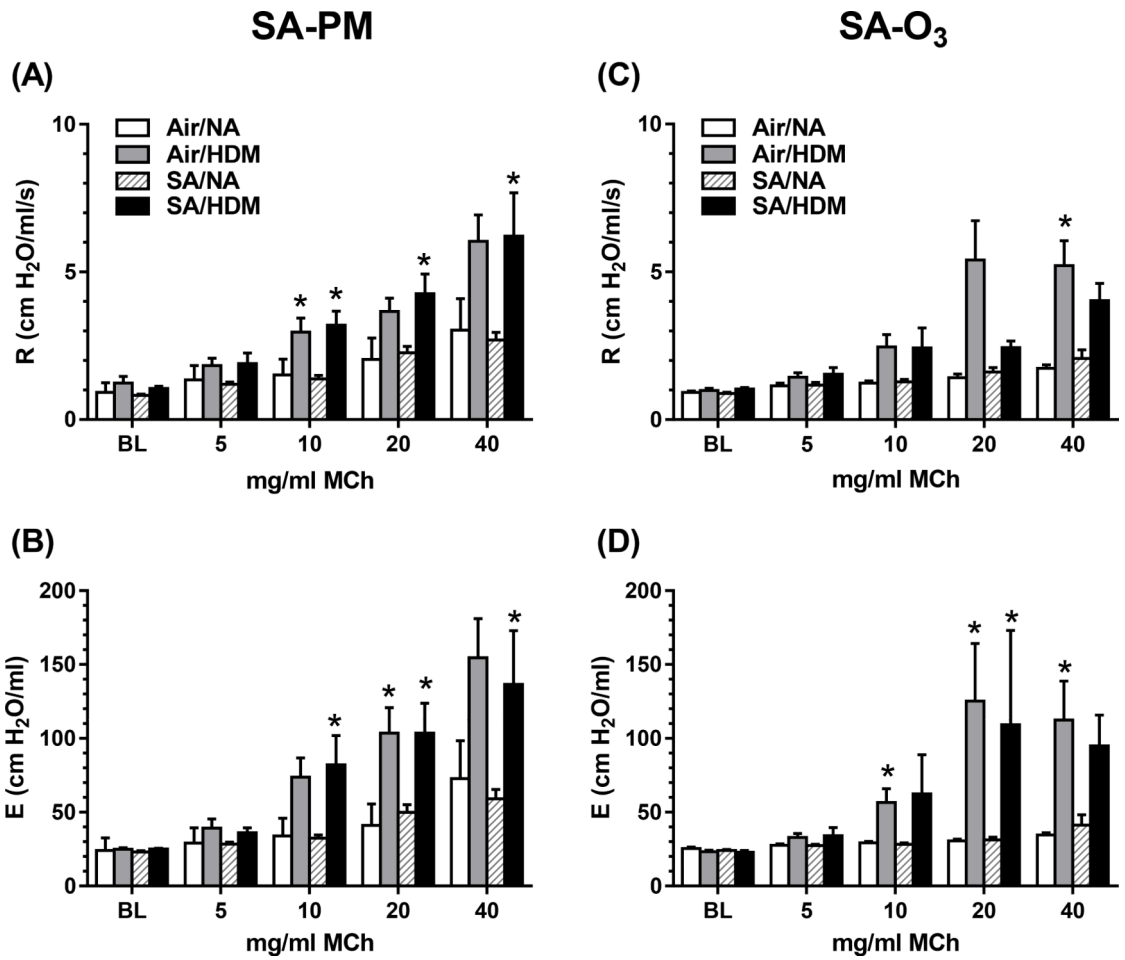

Figure 4. Exposure to SA does not exacerbate airway resistance or elastance in HDM-allergic mice.

Airway responsiveness to MCh aerosol challenge evaluated in mechanically ventilated non-allergic (NA) or HDM-allergic (HDM) mice 1 day after 5-day exposure to SA-PM (panels A, B) or SA-O_3 (panels C, D). Data show mean + SEM (n=7–8/group) of lung resistance (R) and elastance (E) at baseline (BL) and after aerosolization of 5, 10, 20 and 40 mg/ml MCh. *P<0.05 *vs.* non-allergic control at the same MCh dose.

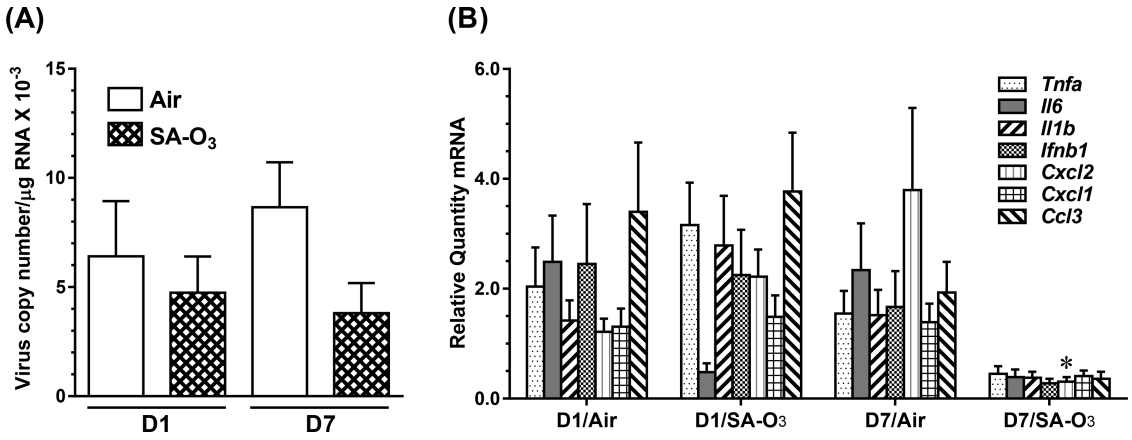

Figure 5.

Virus burdens (A) and cytokine message (B) in the lungs of mice 7 d after infection with 3000 EID_{50} units of influenza A (H1N1) immediately before the first (D1) or last (D7) of 7 daily exposures (4 h/d) to air or SA-O_3. Data show mean + SEM (n=10/group). *P<0.05 *vs.* air-exposed, D7 infection group.

Table 1.

Criteria pollutant levels in simulated smog atmospheres dominated by particulate matter or ozone (SA-PM and SA-O_3, respectively) for GK diabetic rat model and mouse models of house dust mite (HDM) allergy, response to heat-killed S. pneumoniae (HKSP), and response to influenza A (IA) (H1N1) virus. AQHI: Air quality health index. Data show mean (± SEM for multiple exposure days).

Animal Model	Exposure Type (4 h/d)	Exposure Days	O_3 (ppb)	NO_2 (ppb)	$PM_{2.5}$ (μg/m^3)	AQHI
GK Rat	SA-PM	1	87.3	262.2	1140.3	100.7
	SA-O_3	1	326.4	603.9	443.5	108.2
	SA-PM	5	100.3 ± 1.7	274.5 ± 5.9	1107.9 ± 31.5	100.1 ± 3.1
	SA-O_3	5	369.7 ± 6.7	639.9 ± 5.1	308.7 ± 37.2	108.5 ± 2.9
Mouse HDM	SA-PM	1	74.6	226.7	1049.5	89.2
	SA-O_3	1	355.0	606.8	346.6	104.9
	SA-PM	5	97.1 ± 13.4	241.3 ± 6.3	1069.8 ± 40.6	93.5 ± 3
	SA-O_3	5	371.6 ± 22.9	596.8 ± 26.4	293.3 ± 25.3	101.8 ± 4.7
Mouse HKSP	SA-PM	7	96.3 ± 8.6	251.1 ± 8.2	1066.3 ± 27.6	94.2 ± 2.2
Mouse IA	SA-O_3	7	383.5 ± 10.1	613.2 ± 14.1	167.4 ± 23.2	98.1 ± 3.1